Modal analysis with released load excitation

P. Kurowski, K. Mendrok, T. Uhl
AGH University of Science and Technology, Department of Robotics and Mechatronics,
Al. Mickiewicza 30, 30-059, Kraków, Poland
e-mail: tuhl@agh.edu.pl

Abstract

In this paper, the special case of operational modal analysis (OMA) is considered, with excitation having the character of the released load, i.e. a taut rope, which is loosened rapidly during the measurement. The pretension value of the rope is unknown. The work presents the algorithm for frequency response function (FRF) estimation based on the recorded time histories of the experiment described above. The time history of unmeasured excitation was modelled as an impulse with an estimated amplitude based on recorded responses at reference points. The determination of FRF allows the use of experimental modal analysis (EMA) algorithms to identify a scaled modal model. The developed method was verified by simulation data. The results of EMA carried out based on FRFs with modelled excitation and classic OMA based on recorded time histories were compared.

1. Introduction

Modal Analysis is a basic tool for testing the structural dynamics of mechanical structures [1]. Many common operating structures such as satellites, airplanes, cars, rail vehicles, rotating machinery, sports equipment but also bridges, dams, and tall buildings have to be tested according to their dynamics, which influence operational safety, comfort, and acoustics [2,3,4]. The modal models can be identified using experimental modal analysis, which is a popular tool commonly in use by manufacturers and operators of mechanical structures and equipment. A most popular modal test is based on the excitation of structures and the measurements of responses at many locations on a structure during the test [1]. Using dedicated mathematical tools, parameters of modal models can be estimated. One of the main problems of experimental analysis is the choice of proper excitation, which can excite modes which are under investigation. To identify modal parameters of relatively small and light structures, controlled excitation can be realized using dedicated electromagnetic shakers or even modal hammers, equipped with a force sensor. However, in order to identify the modal model of large and heavy civil engineering facilities, operational modal analysis (OMA) is mainly used [4,5,6]. This is because these structures have a large mass and rigidity, and it is difficult to find a suitable forcing device that would provide controlled and measured excitation. The second reason why OMA is used in place of experimental modal analysis (EMA) is the difficulty in isolating the object from other sources of excitation [7,8]. The tested object is often an element of intensively exploited infrastructure, and its exclusion from traffic for the duration of measurements would generate significant costs and difficulties. Even if it would be possible to take the object out of service, it is still subject to excitation from wind, ground movements, etc., and these cannot be isolated or turned off. Therefore, in modal tests, the operational approach based on excitation generated by the natural operation of the object is most often used. However, this excitation often has a narrow band character and does not guarantee the forcing of all natural frequencies of the object from the tested range. Therefore, in some cases, additional broadband forcing is used, for example in the form of an impulse. When this additional forcing is measured, we are then dealing with operational modal analysis with exogenous input OMAX [9,10], but there are also situations when the additional impulse stimulation is not measured. Then, in principle, the procedure should be identical to OMA. In the presented work, it was assumed that the additional excitation will have the character of the released load, i.e. a taut rope, which is loosened rapidly during the measurement. The pretension value of the rope is not known. This type of measurement is repeated cyclically to compensate for random errors by averaging. There are many different algorithms for modal parameter estimation from operational measurements [12, 13, 14]. The paper presents the algorithm for frequency response function estimation based on the recorded time histories of the experiment described above. The time history of unmeasured excitation was modelled with an impulse with an estimated amplitude based on recorded responses at reference points. The determination of FRF allows the use of EMA algorithms to identify the modal model. The developed method was verified with the use of simulation data. The results of EMA carried out based on FRFs with modelled excitation and classic OMA based on recorded time histories were compared.

2. Released load excitation method

2.1.Assumption

In this paper, we assume that the approach related to forcing particularly large objects through the rapid preload release method can be replaced with a force impulse applied virtually to an object. Such an approach is especially useful in cases where the use of dedicated inductors is very expensive or impractical, and the impulse excitation technique applied agitates the structure insufficiently. It can be used in particular when testing civil engineering structures, where a large proportion of structural elements use steel materials. To carry out such an experiment, it is necessary to make several additional assumptions that will enable the application of the procedure.

Measurement assumptions:

- The measurement of the actual object will take the form of recording response signals to specific forcing.
- Forcing will consist of attaching a rope to the item, pre-tensioning it, and breaking the rope violently.
- The rope pre-tension will not be measured.
- The measurement will not be synchronized with the rope breaking act.
- Vibration acceleration sensors will be mounted in selected places on the structure.
- The sensors will synchronously perform measurements during the experiment.
- To increase the statistical significance of the measurement for each sensor setting, the experiment will be repeated several times.
- If in subsequent partial experiments the measurement sensors are moved, it is necessary to leave at least one point in common for all recordings.
- The sampling frequency should be the same for all measurements.

In this paper, to test the approach, we used simulation data generated based on the model described in paragraph 3. We prepared data in the form of time signals collected during the simulation of the tested digital model. Additionally, the data meets the assumptions presented above. For the simulation, it was assumed that all the necessary measurement analyses will be obtained from a single simulation. This will allow free selection of a benchmark. To improve the estimators, the simulation was repeated seven times. This is equivalent to performing the experiment seven times during the fieldwork.

Two main scenarios for the analysis of measurement data were compared:

1. Operational approach - consisting in determining the function of reciprocal spectral densities. In such a case, operational modal analysis algorithms can be used.
2. Pseudo-impulse approach - consisting in adding an additional standardised impulse signal to measurement data. This approach allows for the estimation of the spectral transition function, which can then be analysed with classical modal analysis algorithms.

2.2.Modal parameter estimation method

The method uses additional information related to the method of forcing the structure. The method consists in getting the item out of its equilibrium state by tensioning the rope attached to it, then suddenly releasing the tension. As a result of such action, after releasing the tension, the structure engages in free vibrations related to the object’s return to the state of equilibrium. From the point of view of the analysis of the measurement data, this situation is identical to the examination of the item's response to impulse forcing. The method assumes that such a pseudo-impulse will be generated and used to stimulate the pseudo-spectrum frequency response function (FRF).

The use of the pseudo-impulse only makes sense if the time data obtained in subsequent partial experiments is accurately synchronized. To achieve such synchronization is was necessary to do the following calculation procedure:

1. Determining the reference waveform, based on which the synchronization will be performed.
2. Determining the synchronization points - intersections.
3. Adding a pseudo-impulse.
4. Determining FRF.
5. Using classical modal analysis algorithms to determine the parameters of the modal model.

We will discuss the whole method later in the article using a simulation example.

3. Simulation model

For the purpose of the verification, a 6 DOF numerical model was created. The system was excited in such a way to simulate the behaviour of the loosened rope. The developed model with 6 degrees of freedom is shown in Figure 1.

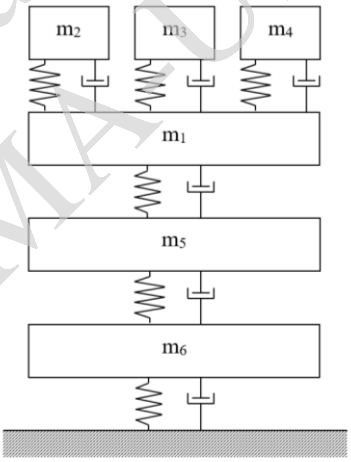

Figure 1. Scheme of the simulation system

The physical parameters of the model are presented in Table 1.

Table 1: Physical parameters of the simulation model

Mass [kg]	$m_1 = 10$; $m_2 = 2$; $m_3 = 3$; $m_4 = 8$; $m_5 = 7$; $m_6 = 6$;

Damping coefficients [N s/m]	c_{12}=3; c_{13}=3; c_{14}=3; c_{15}=5; c_{56}=5; c_{60}=9;
Stiffness coefficients [N/m]	k_{12}=50000; k_{13}=75000; k_{14}=90000; k_{15}=700000; k_{56}=600000; k_{60}=600000;

The following notation was used: the stiffness between the mass *i* and *j* – k_{ij}, the damping coefficient between the mass *i* and *j* – c_{ij}. A viscous damping model was applied.

To calculate the analytical modal model of the system, its equation of motion was formed in the matrix form, and the eigenvalue problem was solved, assuming zero initial conditions for displacements and velocities. As a result, 6 conjugated pairs of system eigenvalues were obtained. On their basis, the natural frequencies and damping coefficients (presented in Table 2) were derived.

Table 2: Modal parameters of the simulation model

MS no.	Natural frequency [Hz]	Modal damping coefficients [%]
1	11.99	0.07
2	20.47	0.22
3	25.16	0.41
4	31.82	0.37
5	61.36	0.24
6	87.55	0.25

This consisted of 7 impulses with random amplitudes and a random inaccuracy of occurrence time. The time history of the excitation signals is shown in Figure 2.

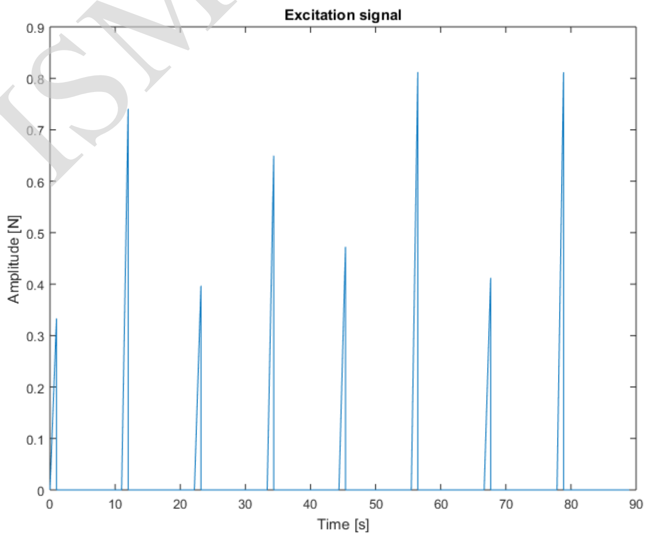

Figure 2: Time history of an excitation signal

4. Analysis of the simulation data

4.1.Operational Modal Analysis

In the operational approach, we used a method usually employed when relying only on system responses related to determining the function of reciprocal spectral densities.

4.1.1.Determination of reciprocal spectral density estimators

We used the periodogram method, with all seven simulation repetitions available to determine the estimators. During the calculation, we ensured that each subsequent averaged frame contained the maximum value of the response signal. This was achieved by triggering a reference response signal and taking synchronous samples from the remaining channels. For the study, we have chosen a signal from mass 1 as a reference. Figure 3 shows the waveform of the obtained estimators of the reciprocal spectral density function. The estimators are clearly smooth, which should ensure the correct estimation of modal parameters.

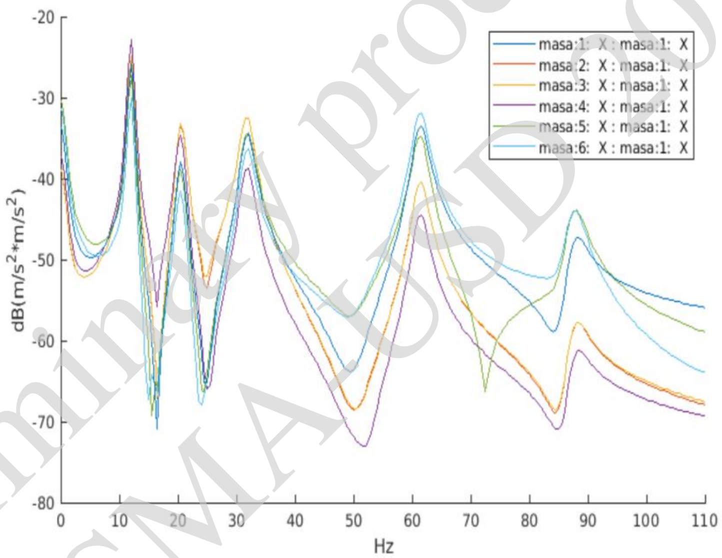

Figure 3: Cross-power spectral densities of the system responses

4.1.2.Modal model estimation

Three different operational modal analysis algorithms were used to estimate the modal model: PolyMax, LSCE, and BR. To achieve the study objective, in each case we used an algorithm for automatic pole selection from the stabilization diagram. Table 3 presents the results of the analyses performed together with their comparison to known parameters of the simulated model.

Table 3: Comparison of modal parameters estimated with the use of consecutive OMA algorithms with nominal parameters.

Model		Polymax		LSCE		BR	
Nat. Freq [Hz]	Modal Damp. [%}	Nat. Freq [Hz]	Modal Damp. [%}	Nat. Freq [Hz]	Modal Damp. [%}	Nat. Freq [Hz]	Modal Damp. [%}
11,99	0,49	11,95	0,36			12,00	1,46
20,47	1,56	20,51	1,94			20,49	2,47
		20,51	3,11				
25,16	2,88						
31,80	2,59	31,85	2,91	31,47	3,27	31,55	3,14
				32,19	2,91	31,86	2,91
						32,27	3,05
61,35	1,65	60,96	1,75	60,90	1,81	61,02	1,72
		61,32	1,76	61,00	1,86	61,72	1,73
		61,71	1,73	61,37	1,99		
				61,50	1,83		
				61,72	1,86		
				62,00	1,69		
87,54	1,75	87,26	1,73	87,19	1,87	87,18	1,84
		87,67	1,73	87,90	1,85	87,55	1,83
						87,90	1,83
						88,03	1,74

This comparison shows that sometimes, the algorithms fail to handle the data correctly. Failure to identify the pole around 25 Hz was observed for all cases. The LSCE algorithm also failed to identify the first pole at 12 Hz. Other algorithms did find this pole, but BR, while correctly identifying its frequency, failed to cope with the value of the modal attenuation coefficient. Above 30 Hz the poles were identified, but unfortunately, the stabilization diagrams were not clear for them, and they stabilized several additional lines near the real pole. These stabilization diagrams are shown in Figure 4.

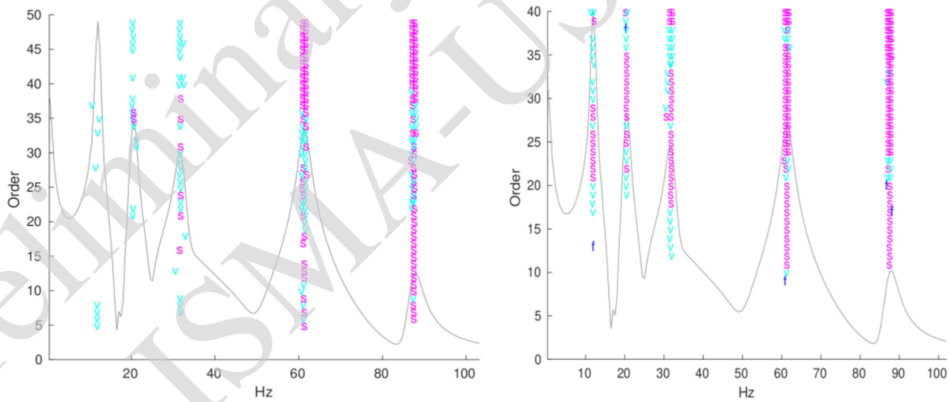

Figure 4: Stabilization diagrams obtained during the estimation of modal model parameters using the Polymax (left) and BR (right) methods.

The waveforms exhibit relatively weak stabilization of the system's initial poles, while for frequencies exceeding 30 Hz, multiple pole lines are stabilized. Noteworthily, the BR algorithm succeeded in stabilizing a 40-degree model, while Polymax needed a 50-degree model. Increasing the degree of the model did not affect the LSCE algorithm's failure to estimate a pole in the area of 12 Hz.

4.2.Experimental Modal Analysis with pseudo-impulse

4.2.1.Determination of the reference waveform

In the classical modal analysis, the selection of the point(s) for energy supply to the system automatically defines reference points. These points should not change their position for the whole measurement session. Forcing signals are also a reference, and allow for normalizing the estimator values. This is not possible in the operational case. The reference points must be chosen arbitrarily. This is also the case here. Out of all the available measurement waveforms, it was necessary to select the point and direction which, for all measurement repetitions, would, first of all, have the best signal-to-noise ratio and, at the same time, would exhibit the steepest slope associated with the increase in response amplitude after releasing the pre-tensioning rope. Fig. 5 shows the system's response at all available measurement points.

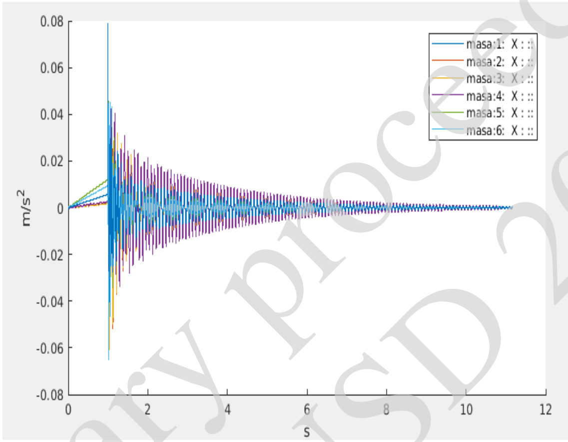

Figure 5: Time histories of responses excited by a single impulse

Due to the nature of the experiment, the signals are of good quality this time, and arbitrary selection of a reference signal is viable. The signal collected from mass 1 was selected for further analysis because of its highest amplitude.

4.2.2.Determination of synchronisation points

One of the assumptions made for the analysis includes a lack of synchronization between data recording and the structure release moment, when it starts to perform free vibrations. This will have a significant impact on the data collected during subsequent repetitions of the experiment. Due to this, individual experiments can be shifted relative to each other.

For synchronization, we used posttriggering. By analysing the maximum amplitudes of all the collected system responses, we assumed the reference level to be 0.02 m/s2. We assumed that a forcing marker would be added 0.005 s before the designated point. Classically, such an operation is associated with putting a pretrigger to the forcing signal.

4.2.3.Pseudo-impulse simulation

The experimental data was collected in seven simulation experiments. Each of the series corresponds to a situation in which an object would be brought out of the equilibrium state and would return to the state of equilibrium by performing free vibrations once the static force is removed. Under experimental conditions, due to differences in the values of the pre-tensioning force putting the system out of equilibrium, the initial free vibration amplitudes may be different in specific measurements. To normalize them, a pseudo-impulse waveform was introduced, whose amplitude depended on the maximum amplitude of the selected reference waveform. Adding a pseudo-impulse for the previously assumed cutting time allows for maintaining phase relationships for all waveforms for a given sample. The introduction of a pseudo-impulse will additionally enable the estimation of FRF, which would significantly improve the quality of the modal parameter estimation.

Generation of a pseudo-impulse should ensure that it “anticipates” the beginning of the slope build-up on all response waveforms. Its generation method must take into account that it must precede the beginning of all response signals. For this experiment, we assumed that its emergence will be additionally advanced by 100 ms.

4.2.4.Estimation of pseudo frequency response functions

Frequency response functions are determined as the system's response to specific forcing. For the analysed system, forcing is simulated with a pseudo-impulse, which in this case, is treated as a forcing signal. The collected responses provide information on the dynamics of the tested object. As a standard, when determining the frequency response function estimator, two approaches can be used to reduce the load on the estimator: averaging in the time domain or averaging in the frequency domain. Averaging in the frequency domain is used for operational measurements for which it is not possible to synchronize the data collected during the experiment, e.g. due to forcing the object with white or coloured noise. A classic example of this type of estimation includes the Welsh method or the periodogram method used for the estimation of spectral density. In this method, the signal is divided into so-called frames. Each of the frames is transformed into the frequency domain using the Fourier transformation, and only after the transformation is it averaged with subsequent frames. Where data synchronization can be guaranteed, it is possible to use averaging in the time domain. For signals containing a large noise component, the time-domain averaging approach may give better signal smoothing effects. In the time-domain averaging approach, the frequency response function estimator is obtained by transforming the already averaged signal. The experiment with forcing the object under investigation with an impulse signal is an example of wide applications of averaging in the time domain. In the presented approach, data synchronization and pseudo-impulse use also allow for applying the time-averaging approach.

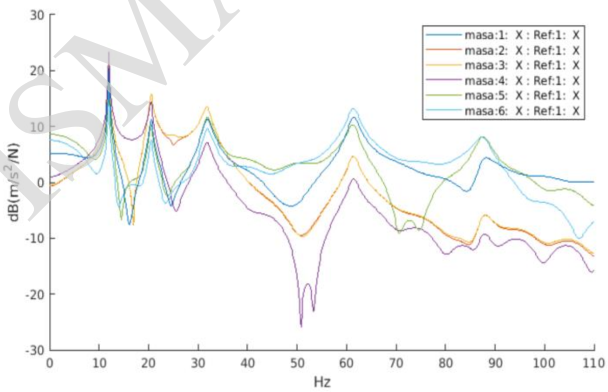

Figure 6: Pseudo frequency response functions of the model.

The spectral transition functions shown in Fig. 6 then served as the basis for the estimation of modal model parameters.

4.2.5.Modal model parameter estimation

In this case, it is possible to use classical modal analysis methods. Please note that the obtained modal model, despite the use of classical modal analysis algorithms, is still not scaled. This is due to the fact that the amplitude of the pseudo-impulse is assumed arbitrarily. It still helps to normalize the waveforms, but does not allow for scaling.

The estimation results are shown in Table 4. They are presented in the frequency range from 0 to 100 Hz. Fig. 7 also presents stabilization diagrams as an indicator relating to the quality of input data for modal analysis procedures. Due to the simulation of the digital model, no visualization of the natural vibration form obtained during the analysis is shown. Additionally, as in estimation with operational modal analysis algorithms, we applied an automatic procedure for the interpretation of the stabilization diagrams.

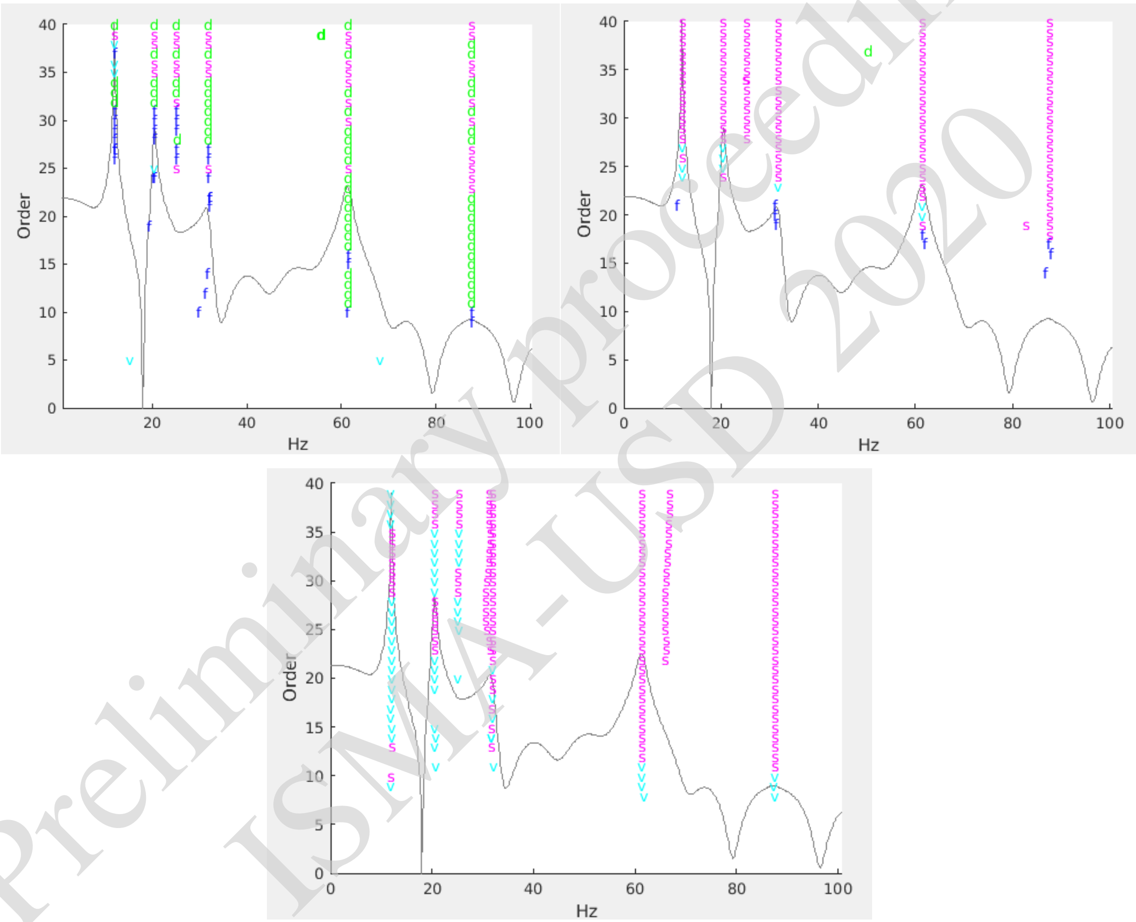

Figure 7: Stabilization diagrams obtained during the estimation of modal model parameters for data obtained using a pseudo-impulse. LSCE algorithm - top row on the left, ERA - top row on the right, LSCF - bottom row.

Table 4: Comparison of modal parameters estimated with the use of consecutive EMA algorithms with nominal parameters.

Model		Polymax		LSCE		ERA	
Nat. Freq [Hz]	Modal Damp. [%]	Nat. Freq [Hz]	Modal Damp. [%]	Nat. Freq [Hz]	Modal Damp. [%]	Nat. Freq [Hz]	Modal Damp. [%]
11,99	0,49	11,99	0,26	11,99	0,50	11,99	0,49
20,47	1,56	20,63	1,00	20,47	1,57	20,47	1,56
25,16	2,88	25,27	2,11	25,14	2,86	25,16	2,88
				25.17	2.90		
		31.34	59.58	31.80	2.60		
31,80	2,59	31,85	2,51	61,35	1,65	31,80	2,59
61,35	1,65	61,35	1,65	61,35	1,65	61,35	1,65
		66.30	59.49	70.53	6.44		
87,54	1,75	87,54	1,75	87,54	1,75	87,54	1,75

It follows from the table that the correct application of the pseudo-impulse influenced the estimation of the modal model parameters. For all the algorithms, we obtained all the 6 poles included in the simulated model. In this breakdown, the ERA algorithm is the most spectacular, as it obtained 100% compliance with the output model, both in terms of the number of poles and their values. The PolyMax algorithm underestimated the parameters of the first three poles in the model, especially in terms of modal attenuation. For both PolyMax and LSCE, there were extra poles in the output set. This is probably due to applying the procedure of automatic interpretation of the stabilization diagram. For the PolyMax algorithm, it should be noted that the redundant poles have very high attenuation coefficients not encountered in the analysis of real objects. Possibly, during object analysis of objects in the course of the actual experiment, it will be possible to use this observation as an additional criterion discriminating such poles. For each of the algorithms used, the stabilization diagrams shown in Figure 7 are much easier to interpret compared to estimating with operational algorithms. This also confirms the validity of the pseudo-impulse approach.

5. Summary

Based on the simulation of a simple system with six degrees of freedom, we have proven the possibility of estimating the parameters of the modal model for examining objects for which controlled forcing is too expensive or even impossible due to their dimensions. In such a case, testing based on static load release leads to broadband forcing, which can be modelled with an impulse. We also presented how to conduct an experiment in such a case, and suggested a computational procedure to improve the quality of the determined modal parameters. We also verified these procedures by comparing OMA algorithms, which are employed as a standard in such cases, with a modified procedure based on the use of a pseudo-impulse to enable using EMA algorithms and improve conditions for their application. The results obtained during these experiments prove that this method can be used to study real objects.

References

[1] D.J. Ewins, *Modal Testing; theory, practice and application*, 2nd ed., Research Studies Press Ltd, 2000.

[2] L. Hermans and H. Van der Auweraer, "Modal testing and analysis of structures under operational conditions: industrial applications," *Mechanical Systems and Signal Processing*, vol. 13, no. 2, pp. 193–216, 1999.

[3] J. Bednarz and T.Uhl, "Model - based SHM of power plants rotating machinery," in *Proceedings of the 8th International Conference on Structural Dynamics, EURODYN 2011*, Leuven, Belgium, 2011, pp. 2432-2439.

[4] S. Qian, Y. Wang-Ji, R. Wei-Xin, and L. Ling-Ling, “Application of transmissibility measurements to operational modal analysis of railway, highway, and pedestrian cable-stayed bridges,” *Measurement*, vol. 148, pp. 106880, 2019

[5] A.C. Altunisik, E. Kalkan, F.Y. Okur, K. Ozgan, O.Ş. Karahasan, and A. Bostanci, “Non-destructive modal parameter identification of historical timber bridges using ambient vibration tests after restoration,” *Measurement*, vol. 146, pp. 411-424, 2019.

[6] M. J. Whelan, M. V. Gangone, K. D. Janoyan, and R. Jha, “Real-Time wireless vibration monitoring for operational modal analysis of an integral abutment highway bridge,” *Engineering Structures*, vol. 31, no. 10, pp. 2224-2235, 2009.

[7] R. Pintelon, B. Peeters, and P. Guillaume, “Continuous-time operational modal analysis in the presence of harmonic disturbances,” *Mechanical Systems and Signal Processing*, vol. 22, no. 5, pp. 1017–1035, 2008.

[8] P. Mohant and D.J. Rixen, “Operational modal analysis in the presence of harmonic excitation,” *J Sound Vibration*, vol. 270, no. 1–2, pp. 93–109, 2004.

[9] P. Guillaume, T. De Troyer, C. Devriendt, and G. De Sitter, “Omaxa combined experimental-operational modal analysis approach,” in: *Proceedings of ISMA2006 International Conference on Noise and Vibration Engineering*, Leuven, Belgium, 2006, pp 2985–2996.

[10] E. Reynders, S. François, and G. De Roeck, “Operational modal analysis using ambient support excitation: An OMAX approach,” *IOMAC 2009 - 3rd International Operational Modal Analysis Conference*, 2009, pp. 635-642.

[11] P. Kurowski and J. Bednarz, “Comparison of modal parameters determined in operational conditions by means of the OMA and OMAX method,” in *Proceedings of the 4th European Workshop on Structural Health Monitoring*, 2008, pp. 127-134.

[12] L. Zhang, T. Wang, and Y. Tamura, “A frequency–spatial domain decomposition (FSDD) method for operational modal analysis,” *Mechanical Systems and Signal Processing*, vol. 24, no. 5, pp. 1227–1239, 2010.

[13] R. Randall, J. Antoni, and W. Smith, “A survey of the application of the cepstrum to structural modal analysis,” *Mechanical Systems and Signal Processing*, vol. 118, pp. 716–741, 2019.

[14] S. Gres, M. Döhler, P. Andersen, and L. Mevel, “Kalman filter-based subspace identification for operational modal analysis under unmeasured periodic excitation,” *Mechanical Systems and Signal Processing*, vol. 146, pp. 106996, 2021.